Transient Thermal Characteristics of a Hydrogen Storage Getter Bed: Use of a Simplified Model with Enhanced Accuracy

R. Bhattacharyya
Heavy Water Division, Bhabha Atomic Research Centre, Mumbai, Maharashtra, India.
Email: rupshabhattacharyya1986@gmail.com; rupsha@barc.gov.in

Abstract: Adsorption of hydrogen on certain metals to form a reversible metal hydride has been known to be one of the most compact and safe methods of storing and immobilizing hydrogen gas and its isotopes. Dynamic thermal analysis of a uranium based getter bed for storage of upto 50 gm hydrogen has been performed in this work. The storage bed has been considered as a pseudo-homogeneous batch reactor with an initial charge of hydrogen and uranium. The vessel dimensions have been assumed similar to the metal alloy canisters available commercially for hydrogen storage. Both heating and cooling systems have been considered available for the beds. The model equations consist of a system of ordinary differential equations and constitutive laws. Variation of bed and coolant temperature, gas pressure and other vessel scale parameters with time, while incorporating particle level transport phenomena and their effects, has been evaluated through a simplified analysis. Effect of temperature dependent cooling and heating has also been investigated. The model enables fast and realistic estimates of getter bed performance under different hydriding conditions with emphasis on the total hydriding time.

Keywords: Batch reactor, Dynamic model, Getter bed, Hydriding, Hydrogen storage, Transient characteristics.

I. Literature Survey

The storage of hydrogen gas and its isotopes in the form of a metal or alloy hydride has been proven to be a very effective, safe, compact and low pressure technique for both stationary and automobile applications [1,2]. For storage of hydrogen, a large number of different hydride forming metals and alloys have been extensively studied. Metallic uranium is one of the earliest known elements capable of adsorbing hydrogen at room temperature and low overpressure while releasing it at a temperature of about 430^{o}C and 1 bar pressure [3,4]. This reversible reaction has been extensively studied in the context of hydrogen storage and its kinetic data are available in literature [5,6]. Uranium has also been considered as the reference material for hydrogen isotope storage in fusion energy systems [7], alongside an intermetallic alloy like zirconium cobalt [8].

In the present work, a simplified heat transfer analysis of getter bed vessels for storing different quantities (i.e. up to 50 gm) of hydrogen in the form of uranium hydride has been carried out. While a heavy metal like uranium will not be suitable for on-board hydrogen storage in automobile applications because of the low maximum gravimetric storage capacity of 1.25%, this system is chosen as a representative case to demonstrate the use of a simplified mathematical model for simulation of metal/alloy based getter bed performance for hydrogen storage. The maximum quantity of hydrogen to be stored in a single vessel as a reversible hydride considered here is also commensurate with the expected hydrogen isotope storage capacity of a single vessel based on zirconium alloys for use with fusion reactor systems like ITER [8]. The model equations consist of coupled ordinary differential equations along with kinetic laws and other constitutive equations. Diffusional resistances to hydrogen gas transport to the surface of the metal for reaction have been considered via the use of an effectiveness factor in the intrinsic rate equation of the reaction. These effectiveness factors have been estimated by the author in a previous study, where a single particle undergoing the hydriding reaction was modeled [9]. Thus the particle level reaction-diffusion phenomena have been connected with the gross or macroscopic behaviour of the entire packed getter bed in this model. Hence this model is more accurate and more closely representative of the phenomena actually taking place in a getter bed during the hydrogen storage step. Conditions inside the reaction vessel have been assumed to be pseudo-homogeneous as an additional simplification.

A simple analysis using the model in this study enables one to quickly predict the overall performance of the system under different design and operating conditions, like the dynamic variation of parameters such as bed temperature, gas pressure during the hydriding reaction phase, which are the typical parameters monitored during the actual operation of these storage systems. The vessels here are considered to have provisions for active cooling by water, circulated through a

cooling jacket outside them as well as electrical heating through cartridge type heaters. Both heat supply and heat removal (i.e. by changing coolant flow rate in the jacket) can be functions of the instantaneous bed temperature. Thus the model in this work is an extension of the previously developed model by the author for heat transfer study of getter beds [10]. The model developed here can ultimately be used for design of a temperature control system for the getter bed (which is in essence a batch reactor) through appropriate manipulations of coolant flow rate and heater power output. A schematic diagram of the vessel with its heating and cooling systems is shown in Fig. 1.

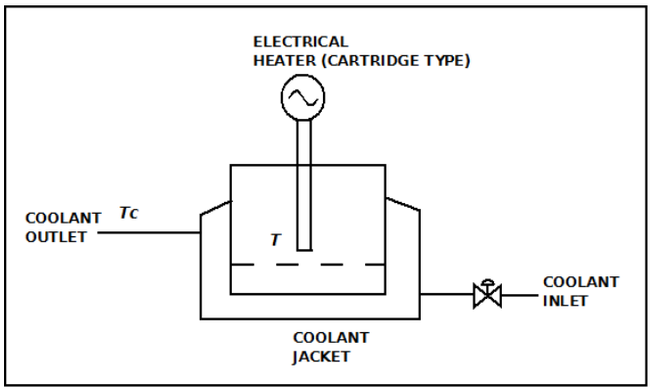

Fig. 1: Representation of the Getter Bed Vessel for Analysis of its Thermal Behaviour

II. Design and Operating Data

The vessel dimensions are so chosen that they match the typical sizes of commercially available solid state hydrogen storage modules or canisters based on lanthanum alloys [11]. This is to enable comparisons of total hydriding reaction time (as well as hydrogen recovery times) when carrying out the reaction in identical sized vessels but while using two different storage materials. The design pressure for each vessel is assumed to be 50 bar (a) and design temperature has been taken as 450°C and these values have been used to determine the vessel wall thickness and the inner diameter of the vessel using Eqn. 1 [12].

$$thk = \frac{P_d D_o}{2\sigma J + P_d} \quad (1)$$

In order to accommodate the volume expansion of metallic uranium during the hydriding process, it is assumed that a maximum of 60% of the internal volume of the vessel will be charged with uranium metal and this will govern the maximum possible hydrogen storage capacity of a vessel of given dimensions. The cooling jacket has been assumed to have an inner diameter 0.1 m greater than the vessel outer diameter and its length is taken to be the same as that of the storage vessel.

The particle size and shape of the metal govern the surface area available for the hydriding reaction as well as the pyrophoric tendency of the metallic particles. In this work, the particles are all assumed to be uniformly sized spheres having diameters from 1.6 to 12 mm. The lower limit is set by the maximum particle size of uranium that can be handled in open air at ambient conditions without the danger of pyrophoricity [13].

The bed considered in this study is operated by charging a certain known amount of hydrogen into the vessel and it is then allowed to react with metal till the pressure drops down to the equilibrium pressure at the operating temperature. At this point the hydriding reaction stops. Thus the getter bed is considered to be a batch reactor. The heat release rate during hydriding is governed by the amount of hydrogen introduced and the kinetics of the hydriding reaction. This in turn is affected by the amount of cooling provided since that affects the reaction temperature. The pertinent data used for solution of the model equations, described in the next section, are reported in Table I and the typical vessel sizes considered in this work are described in Table II.

Table I: Pertinent Data for Model Equations

Parameter	*Value*
k_o	0.51 [5,6]
E_a	25216 J mol^{-1} K^{-1} [5,6]
d_p	1.6-12 mm
S_s	$0.3141/d_p$ m^2 gm^{-1} [13]
ρ_{Updr}	8000 kg m^{-3} [14] -97 kJ mol^{-1} [15]
A	11.492 [16]
B	4471 K [16]
Cp_{H2}	14.4 kJ kg^{-1} K^{-1} [17]
Cp_U	0.12 kJ kg^{-1} K^{-1} [18]
C_{pw}	0.5 kJ kg^{-1} K^{-1} [19]
k_f	W m^{-1} K^{-1} [20]
k_s	1.5 W m^{-1} K^{-1} [21]
k_w	45 W m^{-1} K^{-1} [22]
σ	65 MPa [12]
P_d	$50*10^5$ Pa

Table II: Vessel Dimensions for Storing Different Amounts of Hydrogen [11]

Vessel Number	*OD of Vessel (mm)*	*ID of Coolant Jacket (mm)*	*Vessel Length (mm)*	*Wall Thickness (mm)*	*ID of Vessel (mm)*	*Internal Volume (m^3)*	*Mass of Uranium Loaded (gm)*	*Maximum Hydrogen Storage Capacity (gm (NL))*
1	21	41	100	1	19	$2.97*10^{-5}$	142.6	1.797 (19.97)
2	32	52	200	1.2	29.6	$1.38*10^{-4}$	662.4	8.346 (92.74)
3	32	52	270	1.2	29.6	$1.86*10^{-4}$	892.8	11.249(124.99)

Vessel Number	*OD of Vessel (mm)*	*ID of Coolant Jacket (mm)*	*Vessel Length (mm)*	*Wall Thickness (mm)*	*ID of Vessel (mm)*	*Internal Volume (m^3)*	*Mass of Uranium Loaded (gm)*	*Maximum Hydrogen Storage Capacity (gm (NL))*
4	60	80	225	2.2	55.6	$5.45*10^{-4}$	2616.0	32.961(366.24)
5	60	80	280	2.2	55.6	$6.79*10^{-4}$	3259.2	41.065(456.29)
6	62	82	325	2.3	57.4	$8.41*10^{-4}$	4036.8	50.864(565.15)

III. Model Equations and Solution Algorithm

A simple mathematical model of the hydriding reaction in the getter bed involving overall material and energy balances in the form of ordinary differential equations and using thermophysical properties and kinetic data from literature, was formulated and solved numerically in order to simulate the vessel's unsteady state performance. The details are presented in the following sections.

A. Model Equations

The bed was modeled as a batch reactor with initial charge of uranium inside at a given initial temperature, followed by introduction of requisite quantity of hydrogen gas. No reaction was assumed to occur during the gas filling stage. The entire amount of gas that can be theoretically loaded on to the uranium charged in the vessel was assumed to be filled in at once in the empty volume of the vessel, as opposed to charging several pulses of gas till saturation of the solid occurs. This enabled the calculation of the initial fill pressure of the gas. It was assumed that the reaction could start at ambient temperature itself and the solid getter material was in a sufficiently surface-activated condition prior to gas filling. A pseudo-homogeneous model was taken to describe the conditions inside the getter bed vessel at any time. Thus, inside the vessel, gas and solid were assumed to have the same temperature. Heat transfer from the bed to the coolant flowing in the outer jacket was modeled through the use of an overall heat transfer coefficient that accounts for radial heat transfer through several thermal resistances in series. The inlet temperature and flow rate of coolant were assumed constant, though a temperature control system might be used to modify the flow rate depending on the isothermal temperature required to be maintained during a particular hydriding run. The power input from the heater was modeled as a heat source term in the energy balance equation. This input term will be bed temperature dependent and hence dynamic if a suitable temperature control algorithm is implemented for the hydriding reactor, otherwise it is taken as a constant. Variation of thermophysical properties of the reactants was considered wherever data were available. The model equations are described below.

Hydriding rate equation, corrected for hydride layer diffusional limitations [5,6,9]:

$$(-r_{H2}) = \eta\left(d_p, T\right) kp^{0.5} S_s \rho_{Updr} \frac{V_{solid}}{V_{bed}} \tag{2}$$

The value of η varies throughout the hydriding reaction and it is strongly dependent on particle size, as shown by the author in a previous work [9]. In this work, based on the initial particle size of uranium assumed, an average value of η has been calculated and used to represent the hydride layer diffusional resistance over the entire course of the hydriding reaction.

Overall mole balance on hydrogen gas:

$$\frac{dn_{H2}}{dt} = (-r_{H2}) V_{bed} \tag{3}$$

Overall energy balance [23]:

$$\frac{dT}{dt} = \frac{U_o A_s (T - T_c) + (-r_{H2} V_{bed})(-\Delta H_{Rx}) + q_s}{\sum n_i Cp_i} \tag{4a}$$

The initial conditions were designated as:

$$At\ t = 0, p = P_o\ and\ T = T_o \tag{4b}$$

Equilibrium pressure of hydrogen over uranium is expressed as a function of temperature as follows [16]:

$$\ln P_{eq} = A - \frac{B}{T} \tag{5}$$

The wall heat transfer coefficient was calculated from Eqns. 6, 7, 8 using a particular initial diameter of the spherical particles (1.6 - 12 mm) [24] to account for radial heat transfer. Axial heat transfer was neglected in this analysis by assuming perfect insulation along the longitudinal direction. The bed voidage was evaluated from Eqn. 9 [25].

$$Nu_w = \frac{h_w d_p}{k_f} = 2.4\left(\frac{k_e^o}{k_f}\right) + 0.054\left(1 - \frac{d_p}{D_i}\right) Re_p Pr^{1/3} \tag{6}$$

$$\frac{k_e^o}{k_f} = \left(\frac{k_s}{k_f}\right)^m \tag{7}$$

$$m = 0.28 - 0.757 \log(\varepsilon_b) - 0.057 log\left(\frac{k_s}{k_f}\right) \tag{8}$$

$$\varepsilon_b = 0.4 + 0.05\left(\frac{d_p}{D_i}\right) + 0.412\left(\frac{d_p}{D_i}\right)^2 for \frac{d_p}{D_i} < 0.5 \tag{9}$$

The thermal conductivity of the getter material strongly influences the wall heat transfer coefficient. Bulk metallic uranium has a much higher thermal conductivity than the uranium hydride and uranium chips or powder, a mixture of which is what will be found in the getter bed at any time during the hydriding reaction. Thus the bed thermal conductivity is assumed to be, on an average, 1.5W m^{-1} K^{-1} throughout the course of the reaction [21].

The overall convective heat transfer coefficient U_o based on outside area of the vessel was then calculated as in Eqn. 10, considering resistance of the packed bed, the steel wall and

the flowing coolant to which there is forced convection heat transfer [26]. Heat losses from the jacket surface are neglected and the entire heat generated during hydriding is carried away by the coolant fluid.

$$\frac{1}{U_o A_s} = \frac{1}{h_w A_i} + \frac{ln\left(D_o / D_i\right)}{2\pi k_w L} + R_f + \frac{1}{h_o A_s} \tag{10}$$

The coefficient h_o is calculated from convective heat transfer coefficient correlations for pipe flow, using the equivalent pipe diameter calculated from the vessel outer diameter and the jacket inside diameter. Eqn. 11 shows the correlation used [27]:

$$h_o = 4200(1.35 + 0.02 * tc)\, u_t^{0.8} / D_e^{0.2} \tag{11}$$

The reaction rate constant is obtained from an Arrhenius relationship as shown in Eqn. 12 [5,6]

$$k = k_o \exp\left(-\frac{E_a}{RT}\right) \tag{12}$$

Values of parameters used in the model equations are shown in Table II. The equations were solved for each vessel whose geometric details are presented in Table II.

The thermal energy accumulation term of the coolant was neglected and its outlet temperature at any time, at a constant flow rate, was calculated as [23]

$$T_c(t) = T(t) - \left(T(t) - T_{ci}\right) \exp\left(-\frac{U_o A_s}{m_c C_{pc}}\right) \tag{13}$$

Coolant (i.e. liquid water) properties were assumed as follows [28]:

$$\rho_c = \begin{pmatrix} -2.2911 * 10^{-12} tc^4 + 6.6474 * 10^{-10} tc^3 - 7.9237 \\ * 10^{-8} tc^2 + 4.1465 * 10^{-6} tc + 9.4626 * 10^{-4} \end{pmatrix}^{-1} \tag{14}$$

$$\begin{aligned} C_{pc} = {} & 4.4513 - 2.6893 * 10^{-2} tc + 7.713 * 10^{-4} tc^2 \\ & - 9.3379 * 10^{-6} tc^3 + 5.4717 * 10^{-8} tc^4 \\ & - 1.5196 * 10^{-10} tc^5 + 1.6198 * 10^{-13} tc^6 \end{aligned} \tag{15}$$

$$\sigma_c = \left(77.09 - 0.179 tc - 9 * 10^{-5} tc^2\right) / 1000 \tag{16}$$

$$\mu_c = 0.017998 tc^{-0.927} \tag{17}$$

$$k_c = 0.5722 + 1.6775 * 10^{-3} tc - 5.9952 * 10^{-6} tc^2 \tag{18}$$

B. Solution Algorithm

The equations were solved using a simple, explicit finite difference scheme to obtain average bed temperature, composition and pressure profiles as functions of time, as well as the dynamic variation of coolant outlet temperature. The coupled material and energy balance ordinary differential equations were discretized and solved simultaneously to predict values of gas pressure and bed temperature at different time steps after the initial time. For this, Eqns. 3 and 4 were expressed as:

$$\frac{dn_{H2}}{dt} = f\left(n_{H2}, T\right) \tag{19}$$

$$\frac{dT}{dt} = g\left(n_{H2}, T\right) \tag{20}$$

Runge Kutta 4th order solution method for coupled ordinary differential equations was used for numerical integration of the governing differential equations [29]. The following sequence of calculations was carried out to update the values of hydrogen mole number and bed temperature over successive time intervals, starting with the initial conditions, till the completion of the reaction:

$$k_{11} = \Delta t * f\left(n_{H2}(t), T(t)\right) \tag{21}$$

$$k_{21} = \Delta t * g\left(n_{H2}(t), T(t)\right) \tag{22}$$

$$k_{12} = \Delta t * f\left(n_{H2}(t) + 0.5k_{11}, T(t) + 0.5k_{21}\right) \tag{23}$$

$$k_{22} = \Delta t * g\left(n_{H2}(t) + 0.5k_{12}, T(t) + 0.5k_{21}\right) \tag{24}$$

$$k_{13} = \Delta t * f\left(n_{H2}(t) + 0.5k_{12}, T(t) + 0.5k_{22}\right. \tag{25}$$

$$k_{23} = \Delta t * g\left(n_{H2}(t) + 0.5k_{13}, T(t) + 0.5k_{22}\right) \tag{26}$$

$$k_{14} = \Delta t * f\left(n_{H2}(t) + 0.5k_{13}, T(t) + 0.5k_{23}\right) \tag{27}$$

$$k_{24} = \Delta t * g\left(n_{H2}(t) + 0.5k_{14}, T(t) + 0.5k_{22}\right) \tag{28}$$

$$k_1 = \frac{1}{6}\left(k_{11} + 2k_{12} + 2k_{13} + k_{14}\right) \tag{29}$$

$$k_2 = \frac{1}{6}\left(k_{21} + 2k_{22} + 2k_{23} + k_{24}\right) \tag{30}$$

The updated values of moles of hydrogen remaining in the gas space of the getter bed and the temperature after time interval of Δt were finally obtained as follows:

$$n_{H2}(t+1) = n_{H2}(t) + k_1 \tag{31}$$

$$T(t+1) = T(t) + k_2 \tag{32}$$

Gas conversion at any time t was defined as:

$$X = \frac{\left(n_{H2}(t) - n_{H2}(t=0)\right)}{n_{H2}(t=0)} \tag{33}$$

The values of temperature and pressure dependent parameters in the model equations were accordingly updated when pressure/ mole numbers of hydrogen and temperature values were available for a given time step, to be used for the calculations in the next time interval.

C. Effectiveness Factors

The hydriding of uranium particles has previously been described by the well known shrinking core model [9] and it has been determined that the diffusion of hydrogen through the hydride layer to the unreacted metal core surface is the rate limiting step in the overall process. Details of calculations are available in literature [9]. Thus the bulk gas pressure or hydrogen concentration is not directly available for reaction and the rate equation must be corrected for the diffusion effects. This has been done here through the use of a dimensionless effectiveness factor. It is implicitly assumed that the hydride layer remains intact throughout the reaction and does not spall

off from the unreacted core surface. Further, the effectiveness factor has been assumed to be weakly dependent on the bulk gas concentration but it depends on reaction temperature since gas diffusivity through the hydride layer strongly depends on reaction temperature.

The isothermal effectiveness factor for a heterogeneous gas-solid reaction, such as the hydriding of metallic uranium, at a given reaction temperature, has been defined in this study as follows [23]:

$$\eta = \frac{\text{Actual rate of surface reaction on the metal surface of the core}}{\text{Theoretical rate of reaction at the bulk gas concentration and temperature}} \quad (34)$$

The value of η does not remain constant throughput the reaction because the particle size changes as the less dense hydride layer forms around the unreacted core [9]. Moreover it changes because reaction temperature changes during the hydriding run. For a given initial particle size, the time averaged effectiveness factor has been estimated at several different temperatures and best fit equations have been derived for each particle size, as shown in Table III. These expressions have been used in the rate equation, Eqn. 2, to model the hydriding kinetics.

Table III: Effectiveness Factors for Hydriding Reaction of Uranium at Different Temperatures (Bulk Hydrogen Pressure = 10^5Pa)

Particle Diameter (mm)	*Average Effectiveness Factor as Function of Reaction Temperature*
1.6	$1.64*10^{-6}T^2-1.4*10^{-3}T+0.30095$
3.2	$8.67*10^{-7}T^2-7.29*10^{-4}T+0.1558$
6	$4.7*10^{-7}T^2-3.95*10^{-4}T+0.08378$
10	$2.80*10^{-7}T^2-2.33*10^{-4}T+0.04925$
12	$2.2*10^{-7}T^2-1.826*10^{-4}T+0.03880$

Determination of the effectiveness factor separately for different reaction conditions enables one to decouple the phenomena taking place at two different length scales in the same system i.e. at the particle level and at the vessel/reactor level. The particle level phenomenon is thereby simply incorporated into the model equations for the vessel behaviour under dynamic conditions, without having to alternately switch between the sets of equations representing particle level and reactor level behaviors respectively. This decoupling enables one to obtain more realistic and faster estimates of the performance of the hydrogen storage beds.

IV. Parametric Studies and Results

A. Time Step Size Independence Test

The initial few simulations were run by varying the step sizes in order to ascertain the effect of the selected value of Δt on the calculated temperature and pressure profiles as well as the time required for the completion of the simulation. The maximum time step size that could be chosen without significantly altering the computed profiles was identified and used for all subsequent simulations. Fig. 2 shows the variations in the dynamic profiles as a function of time step for certain conditions of vessel design and operation. It was observed that there was only negligible variation in the computed profiles as the step size was decreased from 50 s to 0.5 s but the time taken in computing these profiles depended on the time step size used. The minimum time step was therefore selected to be 0.5 second, since any further reduction in this value did not modify the calculated profiles but only enhanced computational time. This time step was deemed to be sufficiently small and hence accurate as well for capturing minute details of the computed profiles, for a total reaction time of about 5000 s (1.39 h) in the case considered in Fig. 2. This value was used for simulation of all other conditions of getter bed operation.

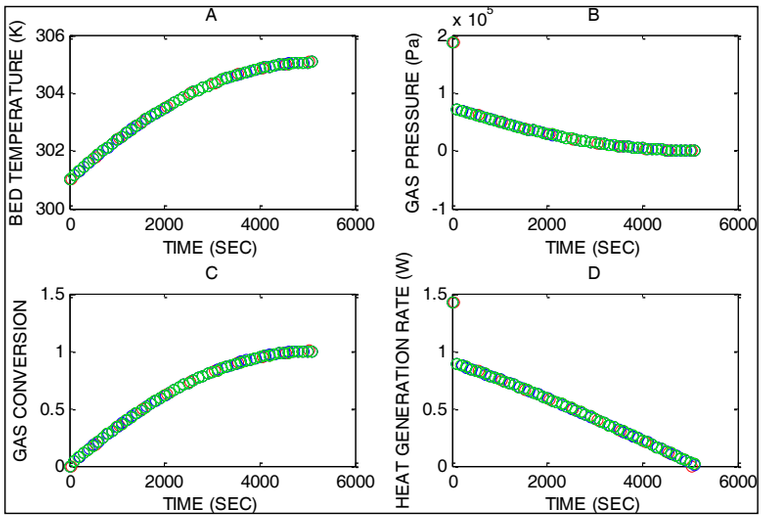

Fig. 2: Calculated Dynamic Profiles of Getter Bed Parameters Using Different Time Steps (d_p = 6 mm, Vessel no. 6, Adiabatic Operation, Δt : **o** 50 s, **o** 10 s, **o** 1.0 s **o** 0.5 s)

B. Adiabatic Operation

The getter bed may be assumed to behave adiabatically when it is well insulated and there is no coolant flow or heat input from the electrical heater. Under such conditions the highest possible bed temperatures and peak heat generation rates during the exothermic hydriding reaction (in absence of external heat input) will be encountered. Thus these represent the most drastic mechanical design conditions for the vessel as well as its cooling system. Setting U_s and q_s to zero in Eqn. 4 reduces the energy balance equation to that required for modeling the adiabatic conditions. The major performance parameters of the vessels under some typical conditions have been summarized in Table IV. The computed dynamic temperature, pressure variation profiles under adiabatic operation with typical parameter values have been shown in Fig. 3. Each vessel has 60% of its volume filled with getter material and the remaining 40% void volume is charged with the theoretical maximum quantity of hydrogen that it can store. This is used to calculate the initial fill pressure of hydrogen.

TABLE IV: PERFORMANCE PARAMETERS OF GETTER BED VESSELS UNDER ADIABATIC CONDITIONS

Vessel Number	*Initial Fill Pressure of Hydrogen (Pa)*	*Initial Particle Diameter (mm)*	*Peak Heat Generation Rate Under Adiabatic Condition (W)*	*Adiabatic Bed Temperature Rise (^oC)*	*Total Adiabatic Hydriding Time (sec)*
1	$1.88*10^5$	1.6	0.71	4.02	364
2	$1.88*10^5$	1.6	3.29	4.12	363.5
3	$1.88*10^5$	1.6	4.45	4.20	363
4	$1.88*10^5$	1.6	13.04	3.92	364.5
5	$1.88*10^5$	1.6	16.22	4.01	364
6	$1.88*10^5$	1.6	20.11	4.06	364
1	$1.88*10^5$	3.2	0.19	4.02	1373
2	$1.88*10^5$	3.2	0.87	4.12	1372
3	$1.88*10^5$	3.2	1.18	4.20	1370
4	$1.88*10^5$	3.2	3.46	3.92	1375
5	$1.88*10^5$	3.2	4.30	4.01	1374
6	$1.88*10^5$	3.2	5.33	4.06	1373
1	$1.88*10^5$	6.0	0.05	4.02	5166
2	$1.88*10^5$	6.0	0.23	4.12	5159
3	$1.88*10^5$	6.0	0.32	4.20	5154
4	$1.88*10^5$	6.0	0.92	3.92	5172
5	$1.88*10^5$	6.0	1.15	4.01	5166
6	$1.88*10^5$	6.0	1.42	4.06	5163
1	$1.88*10^5$	10.0	0.02	4.02	14311
2	$1.88*10^5$	10.0	0.08	4.12	14293
3	$1.88*10^5$	10.0	0.11	4.20	14278
4	$1.88*10^5$	10.0	0.33	3.92	14330
5	$1.88*10^5$	10.0	0.41	4.01	14312
6	$1.88*10^5$	10.0	0.51	4.06	14304
1	$1.88*10^5$	12.0	0.01	4.02	20375
2	$1.88*10^5$	12.0	0.06	4.12	20348
3	$1.88*10^5$	12.0	0.08	4.20	20325
4	$1.88*10^5$	12.0	0.23	3.92	20404
5	$1.88*10^5$	12.0	0.29	4.01	20377
6	$1.88*10^5$	12.0	0.36	4.06	20365

It can be observed that the highest heat generation rates occur for the smallest particle size for any vessel, since under these conditions the highest reaction rates are encountered. This is due, on one hand, to the higher available surface area of the getter material and on the other, to the higher value of the average effectiveness factor. The heat generation rates are not drastically high and they are not likely to pose significant cooling problems for these vessels. For a given vessel, the adiabatic temperature rise during hydriding is identical for all particle sizes and this value of about 4°C is not high. Thus, special cooling arrangements might not be warranted for the appropriately designed getter beds having similar capacities as considered here and air cooling is sufficient. The reaction time in different vessels with the same initial particle size does not vary appreciably, while the peak heat generation rate for the smallest vessel (i.e. one with the lowest storage capacity) is almost 28 times less than the largest vessel considered here. The reaction time in the same vessel for different initial particle sizes also varies considerably because of differing surface area and hence reaction rates during hydriding. The peak heat generation is observed to take place at the start of the hydriding reaction in each case.

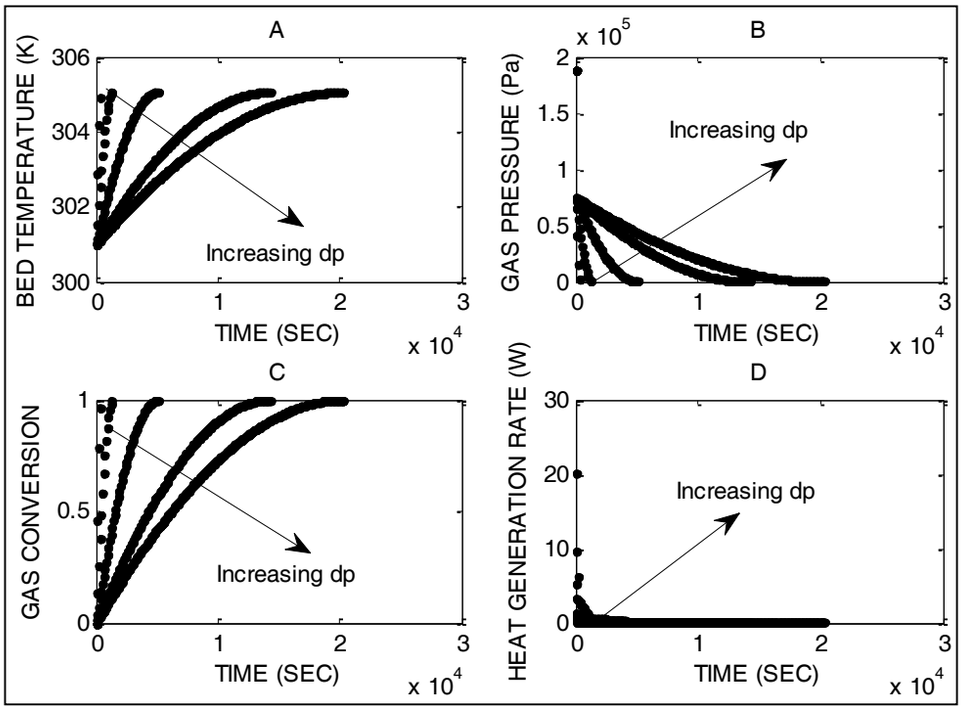

Fig. 3A-D: Simulated Performance Curves of Vessel 6 Under Adiabatic Conditions with Different Initial Uranium Particle Diameter (d_p) from 1.6 mm to 12 mm

C. Operation with Heat Input and Removal

During actual operation of full-scale hydrogen storage vessels based on getter materials, heat removal during hydriding reaction and heat supply during dehydriding are extremely important issues. This section presents the simulated performance results of the getter beds when active cooling by circulating water is provided during hydriding and heat input may or may not be provided in order to take advantage of faster reaction kinetics at elevated temperatures. Faster kinetics is required in keeping with the recommendations of DOE regarding the hydrogen charging or filling time of 3-5 minutes for vehicular applications. The vessels may have different heating and cooling policies, i.e. the coolant flow rate and the heat supply rates may be functions of time and these policies may be implemented by appropriate design and tuning of a temperature control system. Figs. 4 and 5 shows the simulated vessel performance for all the six vessels at a constant coolant flow rate and inlet temperature, without any heat input. It is observed that the temperature of Vessel 1 shows a monotonous decrease with time when coolant flow is provided whereas all the other vessels show an initial temperature rise and then a fall. The heat loss from the vessels is controlled by the cooling water film coefficient since very low water flow rates have been considered sufficient for heat removal. Further enhancing the water flow rate will enable near isothermal vessel operation during hydriding. The peak heat generation rates are quite low and therefore will not present any operational difficulties, even without forced cooling arrangement. Reaction time decreases with increase in vessel size, since the larger beds get the advantage of the initial temperature rise which raises the reaction rates.

Fig. 6 shows vessel performance with a constant heat input and no coolant flow, all other conditions remaining identical to those in Figs. 4 and 5. Heat loss by only natural convection was considered from the vessel in the absence of forced convective

cooling and an outside film coefficient of 5 W m^{-2} K^{-1} was taken for calculation of the overall heat transfer coefficient. Bed temperature is seen to rise in all cases, with the highest temperature being attained by the smallest vessel for the same external heat input (i.e. Vessel 1). Thus reaction time is lowest for this vessel and increases monotonically for the other vessels with increase of internal volume. In order to carry out the hydriding within 5 minutes i.e. 300 s, the heat input rate can be enhanced from the assumed value of 10 W. Different sized reactors will need different constant heat inputs to achieve this goal.

A number of parametric studies were carried out to obtain dynamic profiles of bed performance when either heating or active cooling was provided during the hydriding reaction. Variation in particle size, coolant flow rate and heat input were considered. The graphs showing the simulated performance under different conditions have been included separately under the heading of 'Supplementary Material' at the end of this paper (Figs. S1 to S6).

D. Effect of Different Heating and Cooling Policies

A variety of mathematical functions were chosen to represent the heat input rate into the getter bed vessel as a function of the instantaneous bed temperature. Similarly mathematical representations of the coolant flow rate varying with bed temperature were selected. The effects of temperature dependent heat inputs and coolant flow rates on vessel performance have been shown in this section. Such an analysis is expected to be useful for designing bed temperature control systems.

Let a temperature controller be programmed such that it provides a heater output power, which is a fraction of the maximum output that is directly proportional to the temperature difference between the bed and a set or desired value, and cuts off heat input totally whenever the bed temperature is equal to the desired temperature. This may be expressed mathematically as follows:

$$q_s = q_s^* \frac{(T_{cut} - T(t))}{(T_{cut} - T(t=0))},\ for\ T(t) < T_{cut} \tag{35a}$$

$$q_s = 0,\ for\ T(t) \geq T_{cut} \tag{35b}$$

A few different values of q^*_s were assumed and coolant flow rate was set to zero. The dynamic profiles under these conditions are presented in Fig. 7A-D.

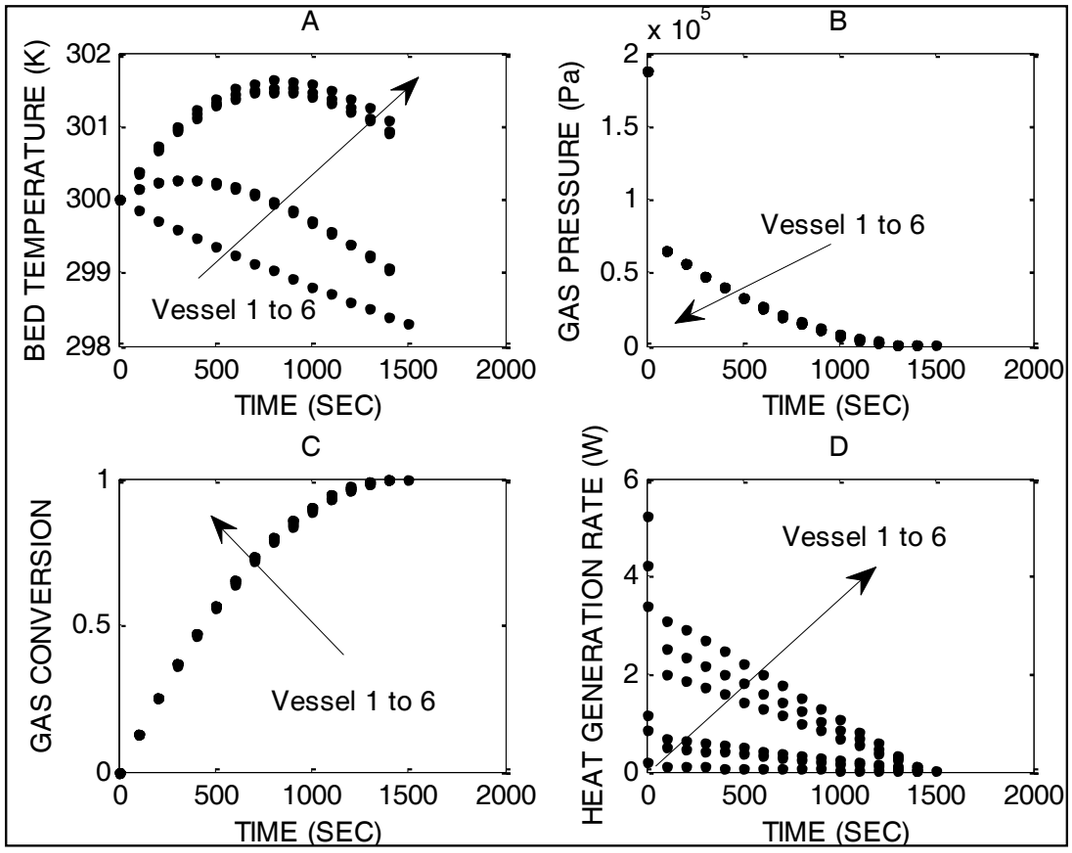

Fig. 4A-D: Simulated Performance Curves of Vessels 1 to 6 for d_p = 3.2 mm and m_c = 0.005 kg/s

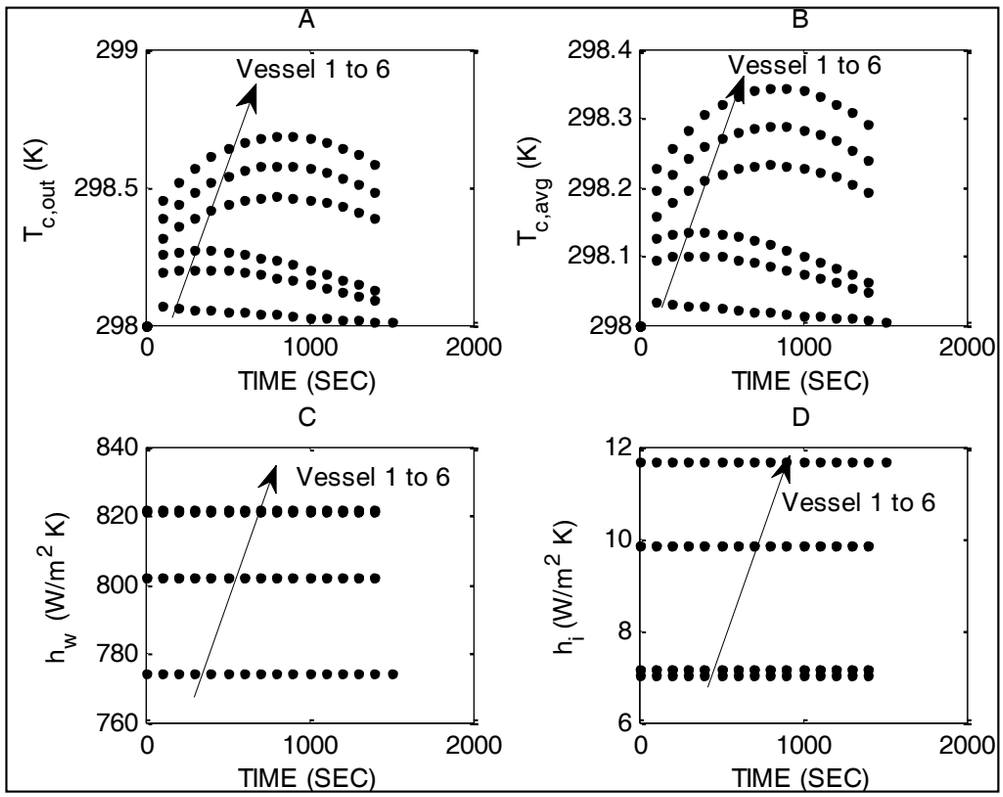

Fig. 5A-D: Simulated Coolant Conditions for Vessels 1 to 6 for d_p = 3.2 mm and m_c = 0.005 kg/s

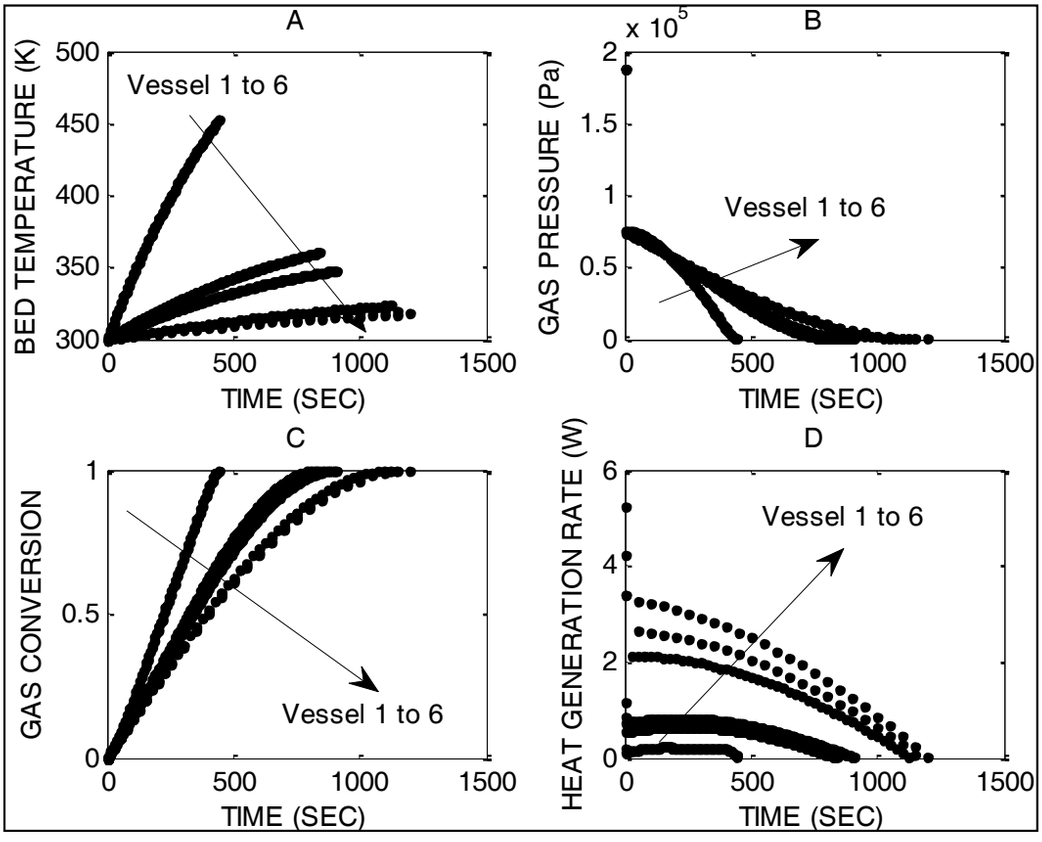

Fig. 6A-D: Simulated Performance Curves for Vessels 1 to 6 with d_p = 3.2 mm, m_c = 0 and q_s = 10 W

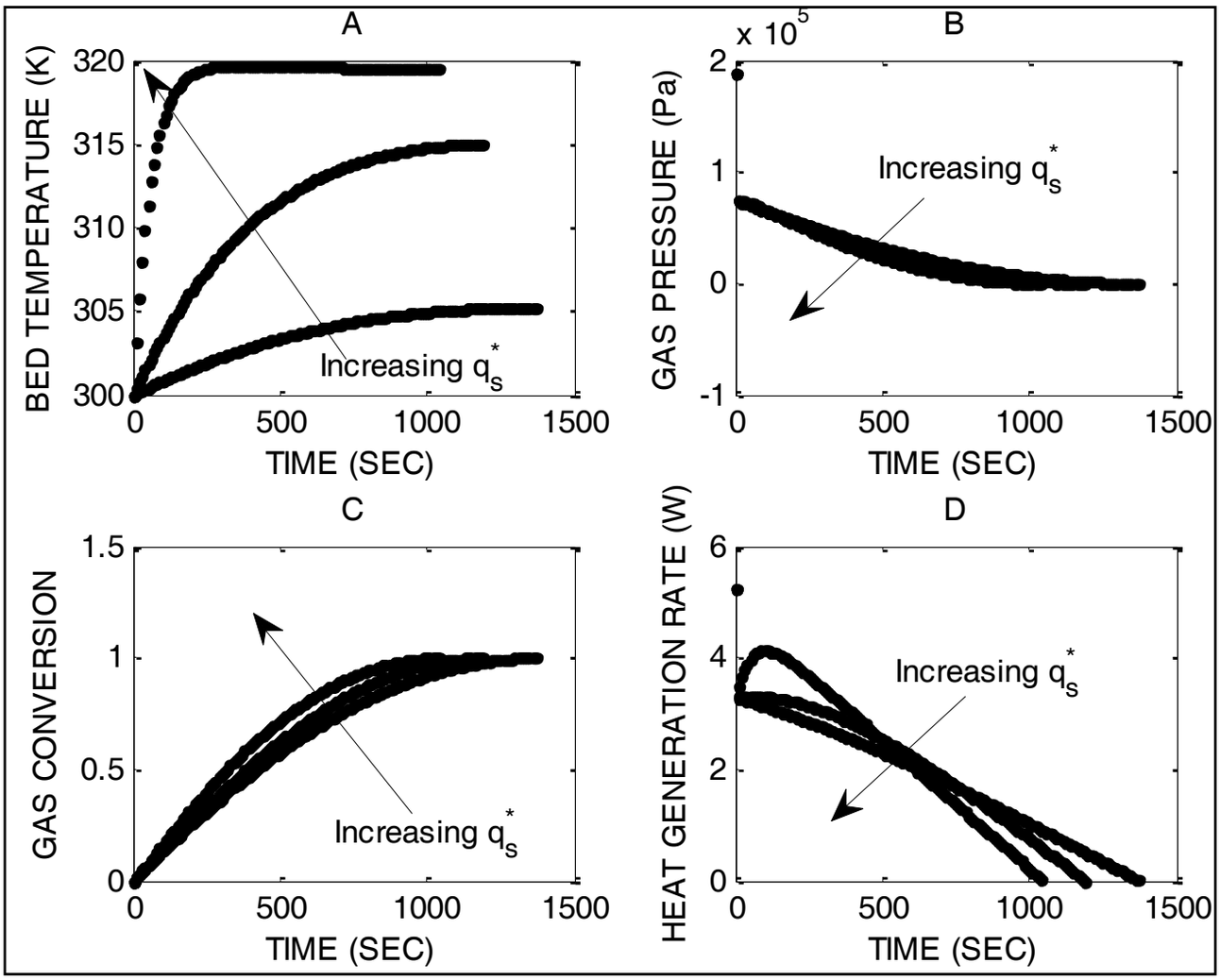

Fig. 7A-D: Simulated Performance Curves for Vessel 6 with d_p = 3.2 mm, m_c = 0 and Linearly Temperature Dependent Heat Inputs (q^*_s= 2, 20, 200 W Respectively and T_{cut} = 320 K)

Yet another example of a temperature dependent heater output, which depends on a pre-selected cut off temperature, could be as follows:

$$q_s = q_s^* * (-0.582) + 0.582 q_s^* \exp\left(\frac{T_{cut} - T(t)}{T_{cut} - T(t=0)}\right), \text{for } T(t) < T_{cut} \quad (36a)$$

$$q_s = 0, \text{for } T(t) \geq T_{cut} \quad (36b)$$

Dynamic bed parameter profiles are generated and presented in Fig. 8A-D for different values of q^*_s in Eqn. 36a-b.

It is observed that depending on the desired temperature to be maintained, whatever is the temperature control algorithm, heaters with low maximum output powers might not be able to reach that temperature value even if it delivers maximum power at all times during the hydriding process. For high output power heaters, once the bed temperature reaches the desired value, the heater supplies only enough power to maintain that temperature and hence a steady temperature profile begins to develop. All other profiles remain time variant and no steady state is attained in course of the reaction. Time required for completion of the hydriding reaction shortens when a temperature programmed heat input is provided but not as appreciably as in the case of a constant power output heater, but the danger of temperature overshoot is minimized by controlled heat input as in the above cases.

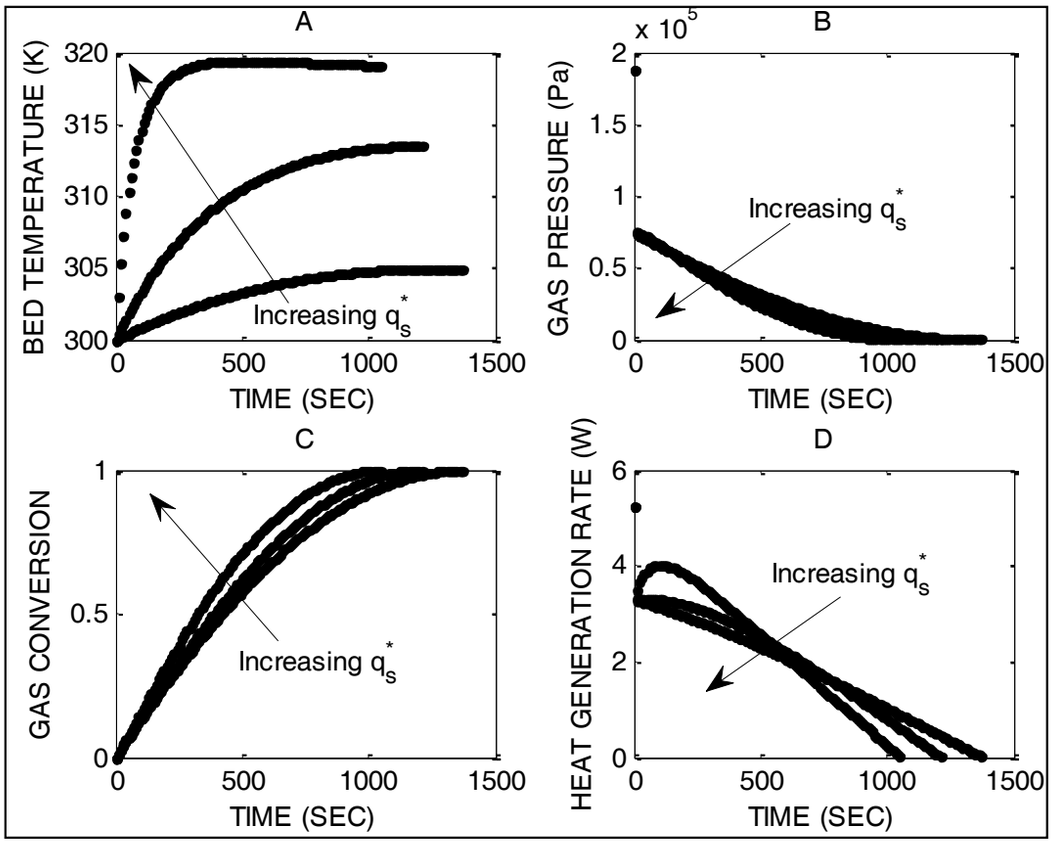

Fig. 8A-D: Simulated Performance Curves for Vessel 6 with d_p = 3.2 mm, m_c = 0 and Exponentially Temperature Dependent Heat Inputs (q^*_s= 2, 20, 200 W Respectively and T_{cut} = 320 K)

Similar to the temperature dependent heat input, the coolant flow rate can also be manipulated on the basis of the instantaneous bed temperature. One possible function could be formulated as follows:

$$m_c(t) = m_c^* \frac{(T(t) - T(t=0))}{(T_{cut} - T(t=0))}, \quad for\ T(t) \le T_{cut} \tag{37a}$$

$$m_c(t) = m_c^*, for\ T(t) > T_{cut} \tag{37b}$$

This algorithm ensures that initially when bed temperatures are low, the coolant flow rate also remains low and it increases linearly in proportion with the temperature rise compared to initial temperature. When this temperature reaches a pre-set maximum value, the coolant flow rate is a maximum. Time required for hydriding is seen to remain almost similar to the cases with constant coolant flow rates and no external heat supply, though differences in bed and coolant temperature profiles are seen. The cut off temperature has been assumed to be 305 K but because this is higher than the maximum temperature rise of the bed in either case, the maximum coolant flow rate is never attained or required. A combination of temperature dependent heating and cooling can thus be used to maintain any set temperature using a programmable temperature controller.

E. Error Analysis

The thermophysical and kinetic data, which were all obtained through experiments by other researchers, used to obtain the dynamic temperature and pressure profiles in the getter bed during hydriding can be assumed to have an error of ± 5 to 10% each. Thus this affects the calculated profiles and the total reaction time. In this section, an estimate of the effect of these errors has been presented. One particular case has been considered as an example. For vessel 6, nominal particle diameter of the getter is taken to be 3.2 mm, initial temperature is 27^{o}C and hydrogen fill pressure is 1.88 bar (a). Adiabatic hydriding is considered. It is assumed that only one of the quantities in Table V is in error in one particular case which leads to some error in the calculated reaction time. Thus this analysis helps identify those quantities which must be known with the greatest accuracy in order to simulate the performance of the storage bed with highest accuracy. This also helps identify those parameters which affect vessel performance most significantly [30].

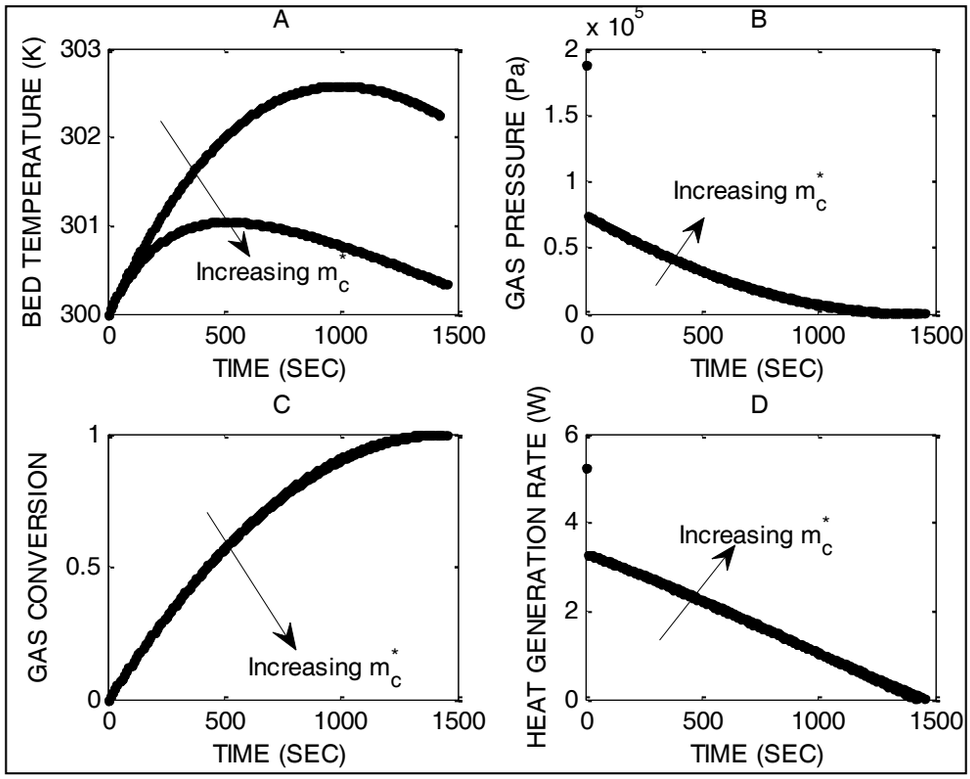

Fig. 9A-D: Simulated Performance Curves for Vessel 6 with d_p = 3.2 mm, q_s = 0 and Bed Temperature Dependent Coolant Flow Rate (m^*_c= 0.0005 kg/s, 0.005 kg/s Respectively and T_{cut} = 305 K)

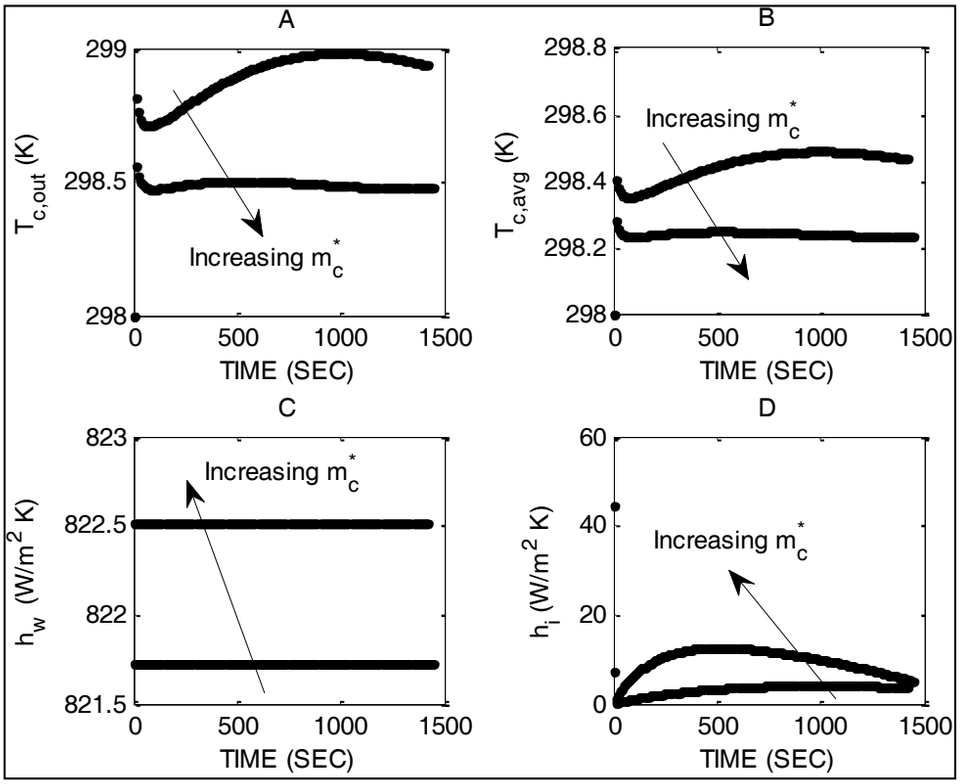

Fig. 10A-D: Simulated Coolant Condition for Vessel 6 with d_p = 3.2 mm, q_s = 0 and Bed Temperature Dependent Coolant Flow Rate (m^*_c= 0.0005 kg/s, 0.005 kg/s Respectively and T_{cut} = 305 K)

Table V: Error Analysis of Getter Bed Performance

Quantity / Parameter	*% Error*	*% Error in Calculated Reaction Time*
Gas thermal conductivity	+ 10%	$< 10^{-4}$
	-10%	$< 10^{-4}$
Gas specific heat	+ 10%	$< 10^{-4}$
	-10%	$< 10^{-4}$
Specific heat of wall material	+ 10%	0.28
	-10%	-0.35
Particle diameter	+ 10%	+10.02
	-10%	-10.02
Density of getter material	+ 10%	-4.94
	-10%	+5.71
Effectiveness factor	+ 10%	-34.76
	-10%	113.71
Thermal conductivity of getter material	+ 10%	$< 10^{-4}$
	-10%	$< 10^{-4}$

It is seen from the Table V that the results of vessel performance simulation are most strongly influenced by the estimates of effectiveness factor used, followed by particle size and getter material density. Gas physical property data are seen to have negligible influence on the predicted profiles and computed reaction time. Specific heat of the vessel's material of construction has some minor effect on the vessel performance because that affects reaction heat absorption by the walls and hence the evolution of the temperature profiles during reaction. Owing to the enormous influence of the effectiveness factor on the vessel performance, it is thus necessary to estimate it most accurately. A mathematical model that separately accounts for the particle level and reactor level phenomena is therefore necessary to simulate the transient behaviour of the getter bed. Bed thermal conductivity and gas thermal conductivity are likely to have significant effect on the reaction time when a non-adiabatic case is considered for analysis.

V. Summary and Conclusion

A simple dynamic mathematical model for simulating the performance of a uranium based getter bed, based on the assumption of pseudo-homogeneous conditions, for storage of up to 50 gm of hydrogen, has been presented in this work. The vessel is assumed to have both heating and cooling arrangements as would be required for full scale hydrogen storage vessels in transport applications, though these vessels would be much larger in size than the ones considered in this study. The vessel dimensions have been chosen to match those of the commercially available rare-earth based hydrogen storage modules. These vessels have been assumed to have 60% of their internal volumes filled with the getter material which is present as uniformly sized spherical pellets of uranium. The entire system has then been modeled as a pseudo-homogeneous batch reactor and its transient performance has been simulated. The performance of the bed under adiabatic conditions has been studied first as an approximation of the most drastic operating conditions which the system is likely to face. The solution for the set of ordinary differential model equations has been obtained by integrating them following the Runge Kutta 4^{th} order algorithm.

For diathermal operation, the various thermal resistances in series in the getter bed have been represented by an overall heat transfer coefficient and it has used in the energy balance equation to account for radial heat transfer from the bed to the coolant. In calculating the wall heat transfer coefficient, a uniform particle size for the uranium turnings has been assumed here but the actual getter material will consist of a variety of sizes and shapes of particles and it is likely to be far from monodisperse. For larger metal chips or turnings, initially the rate of reaction is expected to be very slow because of much lower available surface area for reaction, especially if they are also covered by a layer of uranium oxide or other surface contaminants. This is one situation where a higher initial reaction temperature will be beneficial and thus heat input during hydriding will be required.

The phenomenon of gas diffusion through the growing hydride layer, which has previously been identified as the rate determining step in the overall process [9] has been incorporated into the overall reaction rate through the use of a temperature and particle size dependent average effectiveness factor. Thus particle level and reactor level phenomena have been combined together to arrive at a computationally efficient mathematical model that incorporates the slower overall or global reaction rates rather than the much faster intrinsic kinetics. Through a preliminary sensitivity analysis, this effectiveness factor is seen to strongly influence the computations and therefore it must be known or predicted with much higher accuracy than the other thermophysical data used alongside the model.

The analysis performed here has been used to derive information like peak heat generation rate during hydriding (which must necessarily be the heat load for which the cooling system of the bed has to be designed in case of larger beds), maximum bed and coolant outlet temperature and reaction time under various operating conditions. Reaction times are seen to vary between 0.5 hr to 5.5 hour depending on uranium particle size, presence or absence of heating and cooling and reactor vessel dimensions. Some other studies report complete hydriding times of about an hour for metallic uranium in full scale vessels [31]. This may be considered as a validation of the accuracy of this study which also predicts similar hydriding times. Detailed parametric studies have been carried out to understand the role of various independent parameters on the dynamic behaviour of the vessel. These studies can enable one to optimize the design and operating conditions for the hydriding reactor in such a way that hydriding takes place in a given time e.g. 3-5 minutes as specified by DOE, USA for automobile applications of solid state hydrogen storage systems. Temperature dependent fluid and solid properties have been used wherever relevant. In order to carry out hydriding at a desired temperature, it will be

necessary to manipulate the heat supply and removal rates from the bed, thus the model equations have provisions for including temperature dependent heat input and coolant flow rates. This is the starting point for design of a feedback control system for a hydriding reactor.

In this work, the hydriding of uranium in batch reactors has been simulated. A similar exercise can be carried out for the dehydriding process considering the dehydriding rate equation for uranium. Additionally, the same exercise can be performed for different hydrogen storage getter materials for which the necessary kinetic and thermochemical data are available. Additionally this model may also be used to arrive at the design of a control system for reaction temperature in the getter bed.

Acknowledgements

The author thanks Shri Kalyan Bhanja and Dr. Sadhana Mohan, Heavy Water Division, BARC for encouragement and support while this work was being carried out.

Funding

This research did not receive any specific grant from funding agencies in the public, commercial or not-for-profit sectors.

Conflict of Interest

The author declares no conflict of interest.

Nomenclature

A	Constant in the Van't Hoff equation for hydrogen-uranium system, dimensionless
A_i	Inner surface area of the getter bed, m^2
A_s	Outer surface area of the vessel for heat transfer, m^2
B	Constant in the Van't Hoff equation for hydrogen-uranium system, K
C_{pc}	Specific heat capacity of coolant, J kg^{-1} K^{-1}
Cp_{H2}	Specific heat capacity of hydrogen, J kg^{-1} K^{-1}
Cp_U	Specific heat capacity of uranium, J kg^{-1} K^{-1}
C_{pw}	Specific heat capacity of steel, J kg^{-1} K^{-1}
D_i	Bed inside diameter, m
D_e	Equivalent channel diameter for jacket, m
D_o	Bed outside diameter, m
d_p	Uranium particle diameter, m
E_a	Activation energy for hydriding reaction, J mol^{-1}
h_o	Forced convective heat transfer coefficient in the jacket, W m^{-2} K^{-1}
h_W	Convective wall heat transfer coefficient in packed bed, W m^{-2} K^{-1}
$\triangle H_{Rx}$	Heat of reaction,kJ mol^{-1}
i	Index to component number (i =1 to 3)
J	Joint efficiency, dimensionless
k	Reaction rate constant for hydriding, mol H_2 m^{-2} s^{-1}
$k_{11} - k_{14}$, $k_{21} - k_{24}$	Slope approximations at different time steps using Runge Kutta method of ODE integration, mol s^{-1}/ K s^{-1}
k_1, k_2	Weighted average slope approximations for material and energy balance equations respectively, , mol s^{-1}/ K s^{-1}
k_c	Thermal conductivity of coolant, W m^{-1} K^{-1}
k_o	Pre-exponential factor for hydriding reaction of uranium, s^{-1}
	Thermal conductivity of bed at zero flow, W m^{-1} K^{-1}
k_f	Thermal conductivity of hydrogen, W m^{-1} K^{-1}
k_s	Thermal conductivity of uranium, W m^{-1} K^{-1}
k_w	Thermal conductivity of wall material, W m^{-1} K^{-1}
L	Height of storage vessel, m
m	Empirical index, dimensionless

m_c	Mass flow rate of coolant in jacket, kg s^{-1}
n_i	Number of moles of species i at a given time, dimensionless
n_{H2}	Number of moles of hydrogen at a given time, dimensionless
Nu_W	Wall Nusselt number for the packed getter bed, dimensionless
p	Pressure of hydrogen in the vessel at any time, Pa
P_d	Design pressure of getter bed, Pa
P_{eq}	Equilibrium pressure of hydrogen over uranium, Pa
P_o	Initial pressure of hydrogen over uranium in the getter bed, Pa
Pr	Prandtl number of hydrogen, dimensionless
Pr_c	Prandtl number of coolant, dimensionless
q_s	Heat input into getter bed from the electric heater, W
q_s^*	Maximum electric heater output power into the bed, W
r_{H2}	Rate of hydriding reaction with respect to hydrogen, mol m^{-3} s^{-1}
R	Universal gas constant, J mol^{-1} K^{-1}
R_f	Fouling factor on outside surface of getter bed, m^2 K W^{-1}
Re_c	Coolant Reynolds number, dimensionless
Re_p	Reynolds number, dimensionless
S_s	Specific surface area of uranium turnings or powder, m^2 gm^{-1}
t	Time, sec
tc	Coolant average temperature, ^oC
thk	Vessel wall thickness, m
T	Average bed temperature, K
T_c	Coolant outlet temperature, K
T_{ci}	Coolant inlet temperature, K
T_{cut}	Desired or cut off temperature of the bed user for heater power manipulation, K
T_o	Initial getter bed temperature, K
u_t	Coolant velocity in the jacket, m s^{-1}
U_o	Overall convective heat transfer coefficient based on area A_s, W m^{-2} K^{-1}
V_{bed}	Total internal volume of the vessel, m^3
V_{solid}	Total volume of solid in the vessel, m^3
X	Gas conversion in terms of moles of hydrogen, dimensionless
Δt	Time step, s
ε_b	Bed voidage, dimensionless
η	Effectiveness factor for hydriding reaction, dimensionless
μ_c	Viscosity of coolant, Pa s
ρ_c	Coolant density, kg m^{-3}
ρ_{Updr}	Density of uranium powder, gm cm^{-3}
σ	Maximum allowable tensile strength of SS 316L at 450^oC, Pa
σ_c	Surface tension of coolant, N m^1

References

[1] G. Sandrock, "A panoramic overview of hydrogen storage alloys from a gas reaction point of view," *Journal of Alloys and Compounds,* vol. 293-295, pp. 877-888, 1999.

[2] B. Sakintuna, F. Lamari-Darkrim, and M. Hirscher, "Metal hydride materials for solid hydrogen storage: A review," *International Journal of Hydrogen Energy,* vol. 32, pp. 1121-1140, 2007.

[3] R. Bhattacharyya, and S. Mohan, "Solid state storage of hydrogen and its isotopes: An engineering overview," *Renewable and Sustainable Energy Reviews,* vol. 41, pp. 872-883, 2015.

[4] R. D. Kolasinski, A. D. Shugard, C. R. Tewell, and D. F. Cowgill, *Uranium for Hydrogen Storage Applications:*

A Materials Science Perspective, SANDIA Report, SAND2010-5195, 2010.

[5] M. Balooch, and A. V. Hamza, "Hydrogen and water vapor adsorption on and reaction with uranium," *Journal of Nuclear Materials,* vol. 230, pp. 259-270, 1996.

[6] S. Paek, D. Ahn, K. Kim, and H. Chung, "Characteristics of reaction between hydrogen isotopes and depleted uranium," *Journal of Industrial and Engineering Chemistry,* vol. 8, no. 1, pp. 12-16, 2002.

[7] W. T. Shmayda, "Tritium Processing using Scavenger Beds: Theory and operation," In F. Mannone, (ed.), *Safety in Tritium Handling Technology,* Kluwert Academic Publishers, Ispra (Italy), pp. 23-52, 1993.

[8] T. Hayashi, T. Suzuki, S. Konishi, T. Yamanishi, M. Nishi, and K. Kurita, "Development of ZrCo beds for ITER tritium storage and delivery," *Fusion Science and Technology,* vol. 41, no. 3P2, pp. 801-804, 2002.

[9] R. Bhattacharyya, D. Bandyopadhyay, K. Bhanja, and S. Mohan, "Mathematical analysis of the hydrogen-uranium reaction using the shrinking core model for hydrogen storage application," *International Journal of Hydrogen Energy,* vol. 40, pp. 8917-8925, 2015.

[10] R. Bhattacharyya, K. Bhanja, and S. Mohan, "Heat transfer study of a uranium based getter bed for hydrogen storage," *Chemical Technology: An Indian Journal,* vol. 10, no. 1, pp. 1-17, 2015.

[11] HBank Technology Inc., Metal hydride hydrogen storage for H_2 fuel cells. Available at http://www.hbank.com.tw/Fuel%20Cell%20Application/Hydrogen%20Storage/FC-MH%20Power%20Equivalents.html (last accessed on 4.7.2017)

[12] D. Moss, *Pressure Vessel Design Manual,* 3rd ed., Gulf Professional Publishing, Oxford (UK), pp. 15-16, 2004.

[13] H. B. Peacock, Pyrophoricty of Uranium, DOE Report, WSRC-TR-92-106, 1992. Available at http://www.osti.gov/scitech/servlets/purl/10155050 (last accessed on 4.7.2017)

[14] C. R. Clark, M. K. Meyer, and J. T. Strauss, Fuel Powder Production from Ductile Uranium Alloys, 1998. Available at http://www.iaea.org/inis/collection/NCLCollectionStore/_Public/35/040/35040232.pdf (last accessed on 5.7.2017)

[15] B. M. Abraham, and H. E. Flotow, "The heats of formation of Uranium Hydride, Uranium Deuteride and Uranium Tritide at 25°C," *Journal of the American Chemical Society,* vol. 78, pp. 1446-1448, 1955.

[16] Tritium Handling and Safe Storage, DOE Handbook, DOE-HDBK-1129-2008, 2008.

[17] Gas Phase Heat Capacity (Shomate equation). Available at http://webbook.nist.gov/cgi/cbook.cgi?ID=C1333740&Type=JANAFG&Plot=on (last accessed on 5.7.2017)

[18] D. C. Ginnings, and R. J. Corruccini, "Heat capacities at high temperatures of Uranium, Uranium Trichloride, and Uranium Tetrachloride," *Journal of Research of the National Bureau of Standards,* vol. 39, pp. 309-316, 1947.

[19] Stainless Steel - Grade 316 (UNS S31600). Available at http://www.azom.com/properties.aspx?ArticleID=863 (last accessed on 5.7.2017)

[20] S. C. Saxena, and V. K. Saxena, "Thermal conductivity data for hydrogen and deuterium in the range 100-1100 degrees C," *Journal of Physics A: General Physics,* vol. 3, no. 3, pp. 309-320, 1970.

[21] G. R. Hadley, "Thermal conductivity of packed metal powders," *International Journal of Heat and Mass Transfer,* vol. 29, no. 6, pp. 909-920, 1986.

[22] Austenitic Stainless Steel (316). Available at http://www-ferp.ucsd.edu/LIB/PROPS/PANOS/ss.html (last accessed on 5.7.2017)

[23] H. S. Fogler, *Elements of Chemical Reaction Engineering,* 4th ed., Prentice Hall of India Pvt. Ltd., New Delhi (India), pp. 594-595, 2006.

[24] O. Bey, and G. Eigenberger, **"**Gas flow and heat transfer through catalyst filled tubes," *International Journal of Thermal Science,* vol. 40, no. 2, pp. 152-164, 2001.

[25] W. C. Yang, "Flow through fixed beds," In W. C. Yang, (ed.), *Handbook of Fluidization and Fluid-Particle Systems,* 1st ed., Marcel Dekker Inc., New York (USA), p. 38, 2003.

[26] F. P. Incropera, D. P. DeWitt, T. L. Bergman, and A. S. Lavine, *Fundamentals of Heat and Mass Transfer,* 6th ed., John Wiley and Sons, Hoboken (USA), pp. 571-580, 2007.

[27] G. Towler, and R. K. Sinnott, *Chemical Engineering Design - Principles, Practice and Economics of Plant and Process Design,* Elsevier, p. 827, 2008.

[28] J. G. Collier, and J. R. Thome, *Convective Boiling and Condensation,* 3rd ed., Clarendon Press, Oxford (UK), pp. 583-590, 1996.

[29] S. D. Conte, and C. de Boor, *Elementary Numerical Analysis-An Algorithmic Approach,* 3rd ed., McGraw Hill Book Company, New York (USA), pp. 362-366, 1980.

[30] R. Bhattacharyya, "Theoretical analysis of hydriding reactions of ZrCo and $LaNi_5$ intermetallic alloys using non-isothermal shrinking core model," *Journal of Applied Science and Technology,* vol. 21, no. 1-2, pp. 24-33, 2016.

[31] L. K. Heung, "Tritium transport vessel using depleted uranium," *Fusion Technology,* vol. 28, pp. 1385-1390, 1985.

Supplementary Materials

S1. Extended Parametric Analysis: Graphical Results

S1.1 Effect of Coolant Flow with no External Heat Input

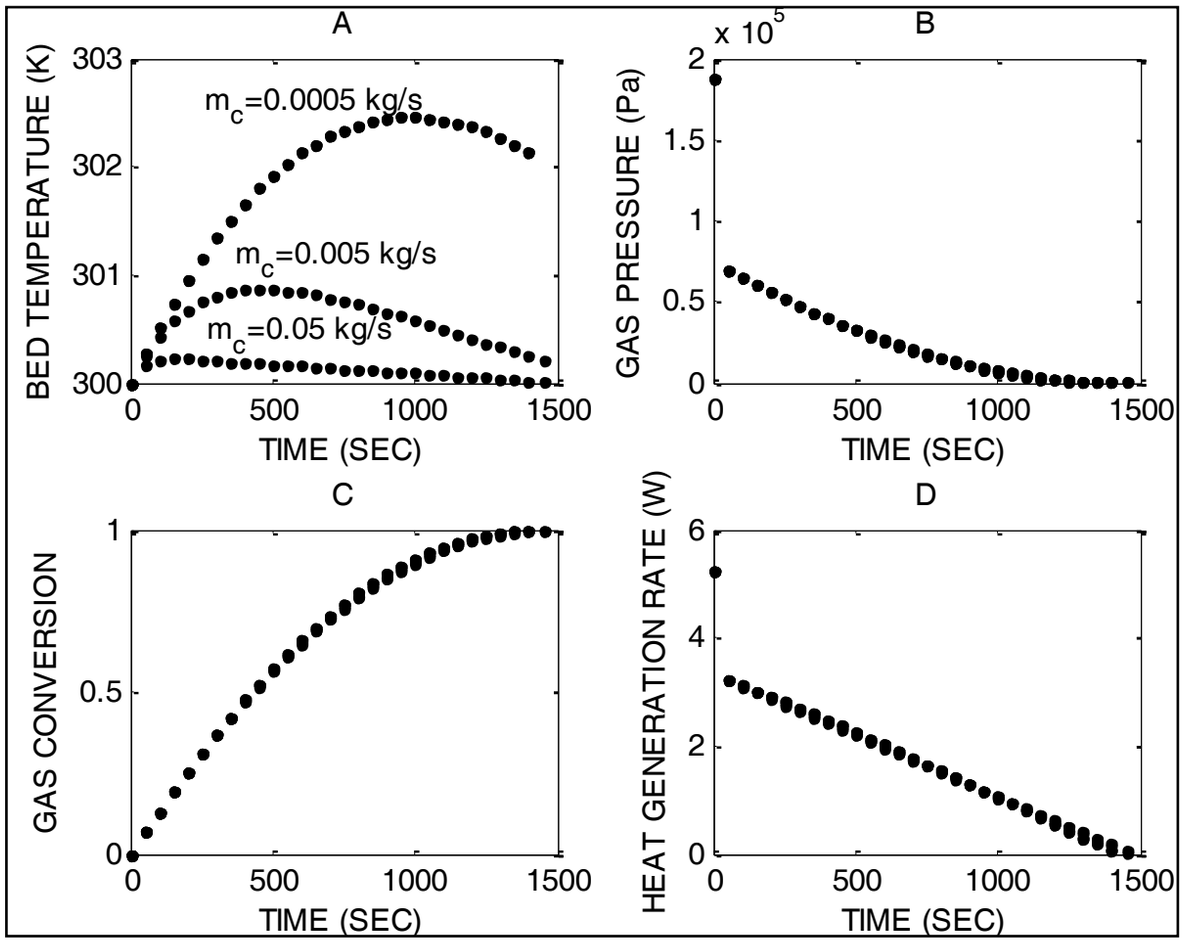

Fig. S1A-D: Simulated Performance Curves for Vessel 6 with d_p = 3.2 mm and Different Coolant Flow Rates

Fig. S1 shows that while the changes in the coolant flow rate affect the evolution of the temperature profile in the getter bed to some extent, it does not lead to much variation in the gas pressure profile or the heat generation profile. This is because of the changes in the coolant heat transfer coefficient which is strongly affected by coolant flow rate and since it is the controlling heat transfer resistance, it affects the temperature pattern in the coolant as well as the vessel, as seen in Fig. S2. Reaction times are not very significantly affected by changing coolant flow rate under the conditions considered in this study.

S1.2 Effect of Particle Size with No External Heat Input

Changes in particle size are seen to strongly affect the temperature and pressure profiles in the getter bed during hydriding since they are directly related to the available surface area for reaction as well as the reaction's effectiveness factors, so they exert a strong influence on the vessel's dynamic behaviour. Reaction times are also significantly affected by changing the particle size of the getter material. In Figs. S3 and S4, it can be observed that doubling of particle size more than doubles the total hydriding reaction time when coolant flow rate is kept constant and no heat input is provided to the bed. Wall heat transfer coefficient practically halves when particle size is doubles yet the coolant film still controls the overall heat loss from the getter bed vessel.

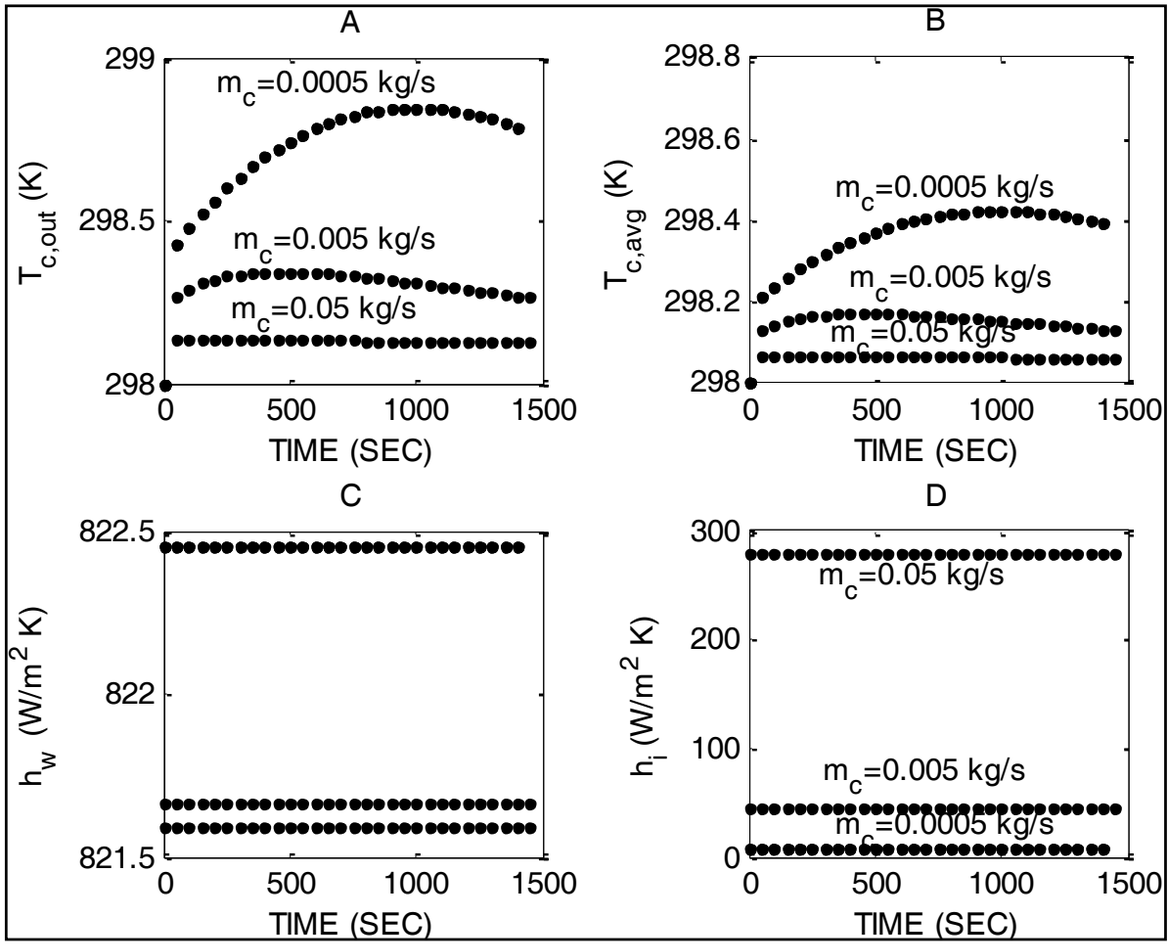

Fig. S2A-D: Simulated Coolant Conditions for Vessel 6 with d_p = 3.2 mm and Different Coolant Flow Rates

S1.3 Effect of Constant Heat Input with No Forced Cooling

For a given particle size of the getter material in a given vessel, adding heat energy to the vessel via electrical heaters can be used to reduce the hydriding reaction time. It is seen in Fig. 5 that for relatively low constant heat inputs of 5 W, 10 W and 20 W to Vessel 6 and heat losses only by natural convection to air, the reaction timesare around 1299 s, 1206 s and 1073 s respectively as opposed to 5000 s for the adiabatic case. This reduction in reaction time is of course attained at the cost of increased bed temperature and the allied operational safety implications arising out of it. Enhancing the heat input by an order of magnitude to 100 W, 150 W and 200 W in the same vessel brings down reaction times to 715 s, 604 s and 503 s respectively. Thus controlled heat input to the getter bed may allow us to tune the reaction time and bring it down to about 300-400 seconds as required for on-board transport applications. An optimization problem may thus be formulated wherein the parameters like getter particle size, initial fill pressure of hydrogen, heat input and removal rate for a given hydrogen storage vessel can be optimally selected with the objective of minimizing reaction time while restricting it to within 300 s and maximum bed temperature to about 50^{o}C which is safe from the handling point of view.

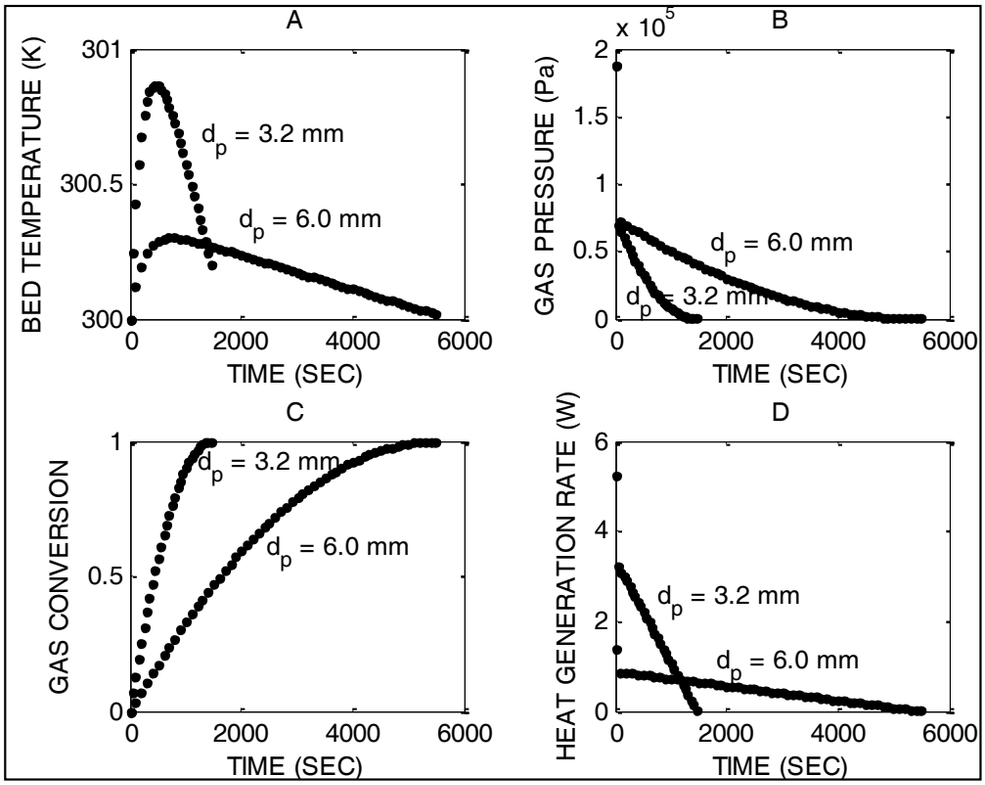

Fig. S3A-D: Simulated Performance Curves for Vessel 6 with m_c = 0.005 kg/s and Different Particle Sizes

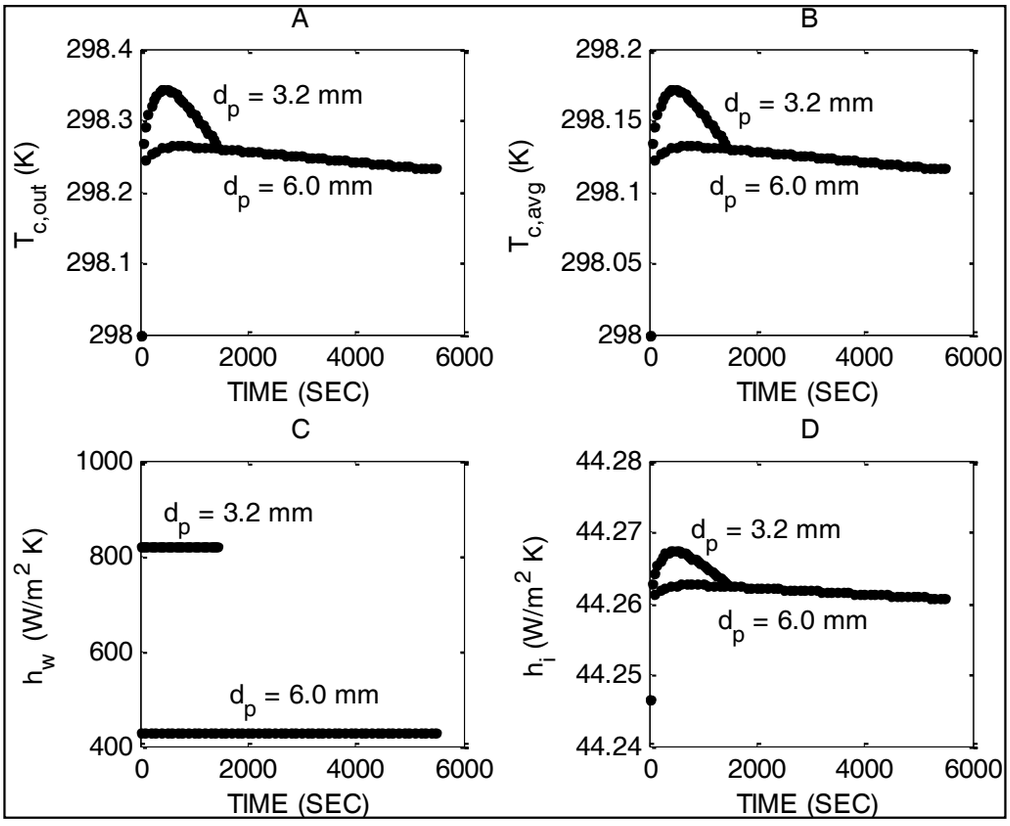

Fig. S4A-D: Simulated Coolant Conditions for Vessel 6 with m_c = 0.005 kg/s and Different Particle Sizes

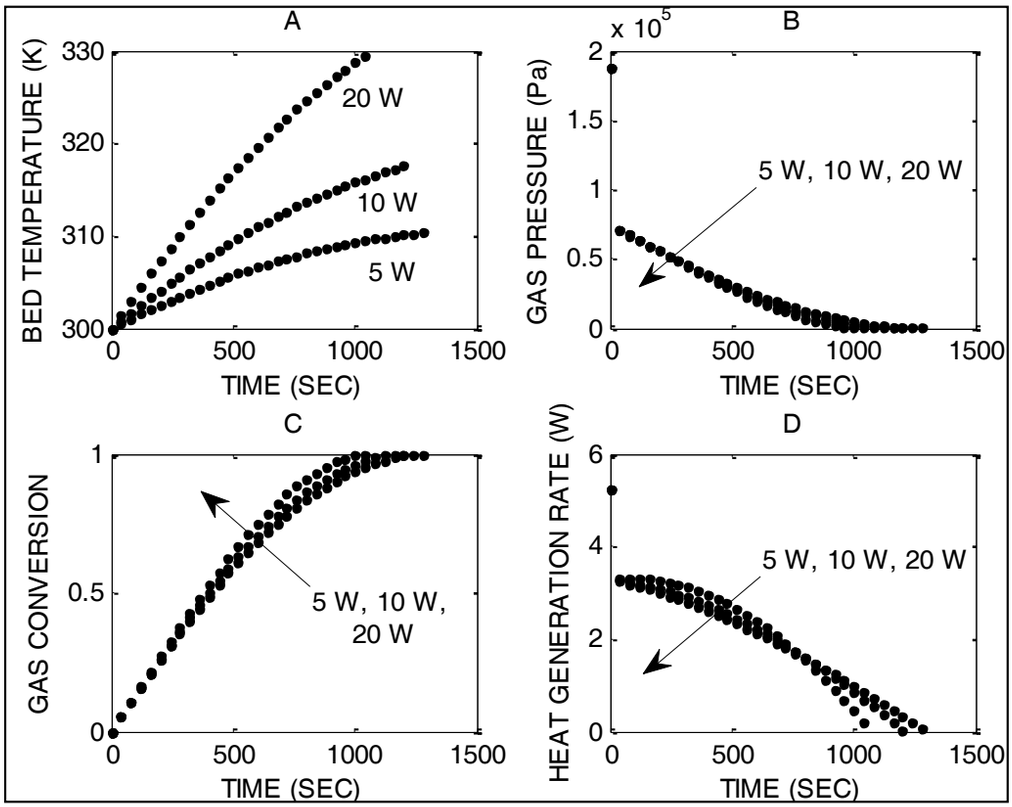

Fig. S5A-D: Simulated Performance Curves for Vessel 6 with m_c = 0.0, d_p = 3.2 mm and Different Heat Inputs (5-20 W)

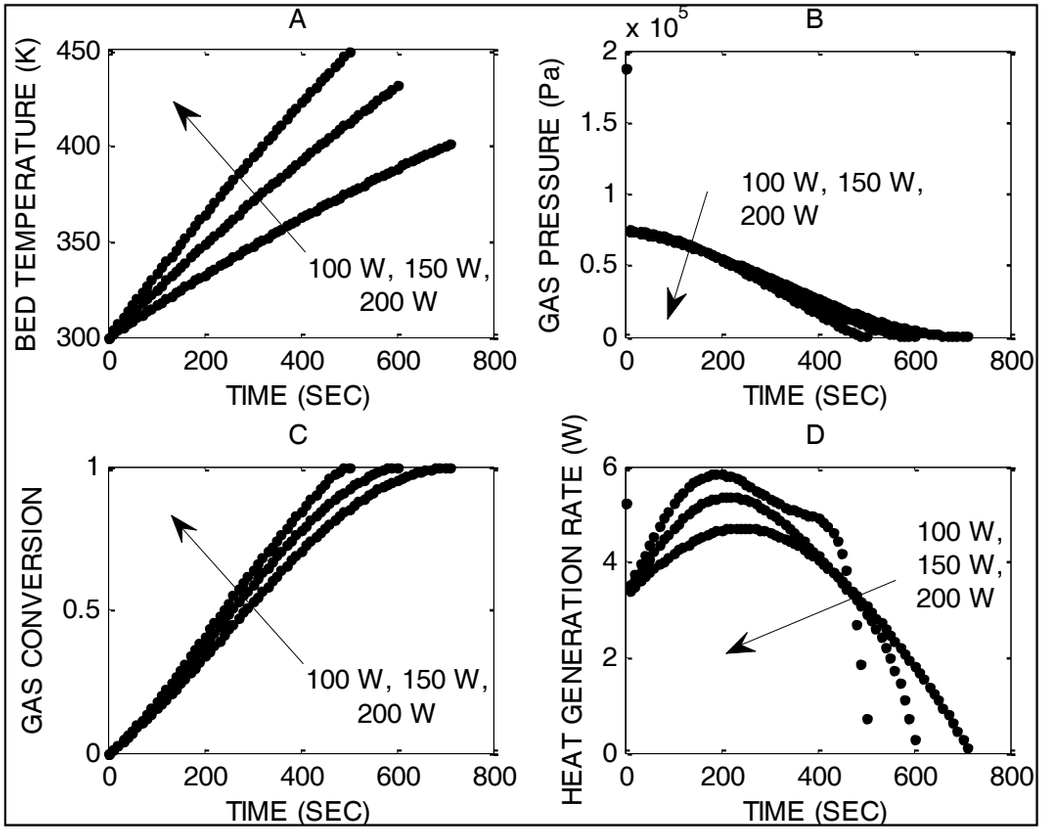

Fig. S6A-D: Simulated Performance Curves for Vessel 6 with m_c = 0.0, d_p = 3.2 mm and Different Heat Inputs (100-200 W)